



# DYNAMIC STIFFNESS FOR STRUCTURES WITH DISTRIBUTED DETERMINISTIC OR RANDOM LOADS

A. Y. T. LEUNG<sup>†</sup>

*The Manchester School of Engineering–Mechanical Engineering, University of Manchester, Oxford Road, Manchester M13 9PL, England. E-mail: [andrew.leung@cityu.edu.hk](mailto:andrew.leung@cityu.edu.hk)*

*(Received 6 August 1999, and in final form 17 July 2000)*

The dynamic stiffness method applies mainly to excitations of harmonic nodal forces. For distributed loads, modal analysis is generally required. In the case of a clamped–clamped beam, the modal decomposition of a uniformly distributed load by the eigenbeam functions inherits slow convergence because the finite loads at the beam-ends cannot be represented efficiently by the zero deflection and zero slope of the clamped–clamped beam functions. The computed reactions at the supports do not converge at all. The problem is eliminated in this paper by using the finite element interpolation functions for the distributed load. If the distributed load is adequately represented, explicit exact solutions are found. Otherwise, the residual load is expanded in the modal space. As the residual modal force is much smaller and agrees well with the clamped–clamped conditions, fast convergence is achieved. By means of the principle of superposition, a structure with members having distributed loads can be analyzed by two systems: one is associated with the individual members having distributed loads and the other is associated with resulting equivalent nodal forces. The required frequency functions are given for all possible cases. The results presented are exact if the load is interpolated adequately by finite element shape functions. Both deterministic and random loads are considered. Closed-form solutions are obtained for the first time.

© 2001 Academic Press

## 1. INTRODUCTION

The dynamic stiffness method [1] employs the solutions of the governing equations under harmonic nodal excitations as shape functions to formulate the analytical stiffness matrix called the dynamic stiffness matrix. The method requires the closed-form solutions of the governing equations which restricts the application areas. A brief introduction of the method and a review is given in section 2. So far, the excitations considered are nodal forces only. Distributed forces will be studied for the first time for both deterministic and random excitations. If the distributed forces can be interpolated adequately by the finite element shape functions, analytical solutions are possible.

The principle of superposition is introduced in section 3 to study a structure with some members having distributed loads. Formulation using an Euler–Bernoulli beam is given as an example. The axial and torsional vibrations are studied in section 4. It is found that the classical modal analysis takes more than a thousand terms to converge to four significant figures for the support reactions if the bar is under the excitation of a uniformly distributed load. The bending vibration is considered in section 5 and it is found that the classical

<sup>†</sup>Present address: Building and Construction Department, City University of Hong Kong, Tat Chee Avenue, Kowloon, Hong Kong.

modal analysis does not give solutions to the support reactions for uniformly distributed load. Formulae for boundary conditions other than clamped-clamped are given in section 6. The method is generalized to other structural members in section 7. The random response is studied analytically in section 8. Finally, numerical examples are presented in section 9.

## 2. THE DYNAMIC STIFFNESS METHOD AND ITS REVIEW

Various methods are available for establishing a mathematical model for the vibration response of structures, among which the finite element method based on static displacements is the most commonly used. There are two forms of the displacement-based finite element method in dynamics. The first, an approximate method, which interpolates the displacements using piecewise polynomial shape functions. The second, referred to as the exact method, which interpolates the displacements using shape functions that satisfy the static equilibrium equations exactly, results in a continuum element. Both forms exhibit inaccuracy since the frequency-independent shape functions fail to represent fully the true eigenfunctions, which depend explicitly on the corresponding natural frequency. The dynamic stiffness method can eliminate such inaccuracy problems by employing the frequency-dependent shape functions that are exact solutions for the governing differential equations, and therefore provides exact natural modes for a vibrating structure. It eliminates spatial discretization error and is capable of predicting on infinite number of natural modes by means of a small number of degrees of freedom. Because the shape functions used are frequency-dependent, the resultant dynamic stiffness matrices  $[\mathbf{D}]$  are inherently frequency-dependent. The eigenproblem for free vibrations or forced vibrations by modal analysis should be replaced by

$$[\mathbf{D}(\omega)]\{\mathbf{u}\} = \{\mathbf{0}\}$$

and

$$[\mathbf{D}(\omega)] = [\mathbf{K}(\omega)] - \omega^2[\mathbf{M}(\omega)],$$

where  $[\mathbf{D}(\omega)]$  is the dynamic stiffness matrix,  $[\mathbf{M}]$  and  $[\mathbf{K}]$  are the global mass and stiffness matrices,  $\{\mathbf{u}\}$  is the nodal displacement vector, and  $\omega$  is the eigenfrequency.

Therefore, the method of dynamic stiffness matrix in vibration analysis of structures has certain advantages over the conventional finite element method, particularly when higher frequencies and higher accuracy of results are required. This is because, in the finite element method, the properties of an individual element are derived from the assumed shape functions and so are not “exact”, whereas the properties obtained from the dynamic stiffness method are based on the closed-form analytical solution of the differential equation of the element and hence are justifiably called “exact”. The disadvantages lie in the transcendental nature of the dynamic stiffness matrix and in the need to solve a non-linear eigenproblem. However, this can be solved without difficulty by means of the Wittrick–William algorithm [2].

The history of the dynamic stiffness method can be traced back to as early as the 1940s with Kolousek’s work [3–6] in which the author calculated the element dynamic stiffness matrix for uniform Euler–Bernoulli and Timoshenko beam elements. Historical notes on the dynamic stiffness method and early references can be found in Akesson’s publication [7] in which he mentioned the works of Gaskell [8], Raithel [9, 10], Veletsos and Newmark [11], Rogers [12], Mohsin and Sadek [13], Armstrong [14], Cheng [15], and Swannell [16].

Later development and applications of the dynamic stiffness method can be found in the works of Afolabi [17], Akesson *et al.* [18, 19], Banerjee and Williams [20], Capron and Williams [21], Chen [22, 23], Curti *et al.* [24], Eisenberger [25, 26], Friberg [27, 28], Hallauer and Liu [29], Hencky [30], Leung [31–40], Lunden and Akesson [41], Ovunc [42, 43], Pilkey [44], Richards and Leung [45], Williams and Kennedy [46], Williams and Wittrick [47], and Zhang and Wu [48] among others. A major advancement of the dynamic stiffness method is made by Leung [1], who was extended the method to a wide range of problems including natural vibration and response analyses, conservative and non-conservative problems, uniform and non-uniform structures, straight and curved members.

A comprehensive literature review on the dynamic stiffness method can be found in Fergusson’s dissertation [49] in which the development and application of the dynamic stiffness method to various kinds of elements and structures are introduced in detail. Some recent development of the method for curved and non-uniform members can be found in Leung *et al.* [50–55] and Eisenberger [56, 57].

3. PRINCIPLE OF SUPERPOSITION

The principle of superposition enables one to study the distributed load on one element beam member at a time and to superimpose the results. Consider the simple structure shown in Figure 1. The structure (a) with a distributed load is equivalent to a clamped–clamped beam (b) plus the structure (c) with equivalent nodal loads only. The equivalent nodal loads equal the reactions of the clamped–clamped beam with their directions reversed.

Therefore for the solution for the clamped–clamped beam under distributed load in harmonic vibration, the distributed load problem of the structure can be solved by the dynamic stiffness method. Usually, the clamped–clamped beam under distributed load is solved by the modal analysis. However, the clamped–clamped beam functions cannot represent the distributed load at the ends of the beam as both the eigenfunctions’ displacements and slopes are zero at the ends. For example, the expansion of the uniformly distributed load in terms of the simply supported beam function is

$$f(x) = \frac{4h}{\pi} \left( \frac{\sin x}{1} + \frac{\sin 3x}{3} + \frac{\sin 5x}{5} + \dots \right), \tag{1}$$

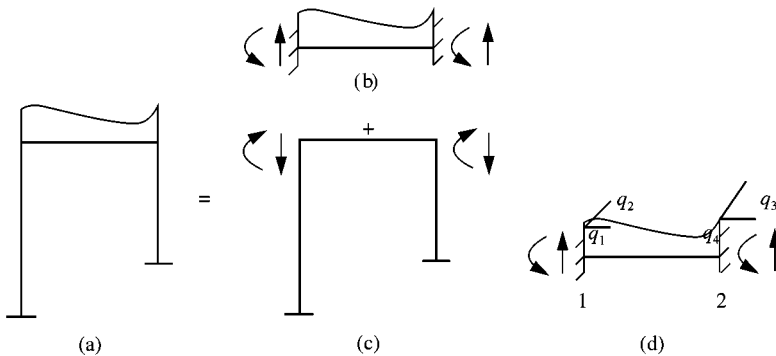


Figure 1. Principle of superposition (a) a simple structure with a distributed load; (b) a clamped–clamped beam with a distributed load; (c) the structures with equivalent modal loads; (d) displacement and slope degrees of freedom.

where  $h$  is the intensity of the load and  $\pi$  is the length of the beam for simplicity. Equation (1) converges extremely slowly to a step function. Alternatively, the distributed load may be expanded into

$$f(x) = [\mathbf{N}(0, x)]\{\mathbf{q}_v\} + \sum \phi_i(x)Q_i, \quad (2)$$

where  $[\mathbf{N}(0, x)]$  is a row vector of the finite element shape functions which are the dynamic shape functions at zero frequency,  $\{\mathbf{q}_v\} = \{q_1, q_2, q_3, q_4\}$  represents the displacement magnitudes and slopes at ends 1 and 2 in Figure 1(d), respectively,  $\phi_i(x)$  is the  $i$ th mode and  $Q_i$  is the intensity of mode  $i$ . For uniformly distributed loads,  $q_1 = q_3 = h$ , the load intensity, and  $q_2 = q_4 = 0$ . Therefore, the load is exactly represented without using natural modes. It is shown below that the end reactions (shears and moments) are simply proportional to the mass matrix if the finite element shape functions are adequate to represent the distributed loads. In general, the finite element shape functions, represented by the first term on the right-hand side of equation (2), take good care of the portion of distributed load at the two ends of a clamped-clamped beam. The residual load conforms very well with the beam functions and the second term on the right-hand side of equation (2) converges rapidly. The deterministic distributed loads are considered first and the random loads are considered later.

#### 4. AXIAL AND TORSIONAL VIBRATIONS OF AN EULER-BERNOULLI BEAM

The governing differential equations and boundary conditions of axial and torsional vibrations of an Euler-Bernoulli beam under harmonic excitations are given, respectively, by

$$EAu'' + \omega^2 \rho Au = -q_u \quad \text{with} \quad u(0) = u(l) = 0 \quad (3)$$

and

$$GJ\theta'' + \omega^2 \rho I\theta = -q_\theta \quad \text{with} \quad \theta(0) = \theta(l) = 0, \quad (4)$$

where  $u$  and  $\theta$  are the vibration amplitudes,  $\omega$  the vibration frequency,  $EI$  and  $GJ$  are the rigidities,  $\rho A$  and  $\rho I$  are the inertia per unit length,  $q_u$  and  $q_\theta$  are the distributed loads per unit length,  $l$  is the length of the beam,  $0 \leq x \leq l$  and a prime denotes differentiation with respect to  $x$ . Since equations (3) and (4) are similar, only equation (3) need to be considered.

It is always possible to express the distributed load of equation (3) as

$$q_u = [\mathbf{n}(0, x)]\{\mathbf{q}\} + \sum Q_i \sin(i\pi x/l), \quad (5)$$

where  $[\mathbf{n}(0, x)] = [1 - x/l, x/l]$  is the finite element shape function matrix,  $\sin(i\pi x/l)$  is the natural mode, and  $\{\mathbf{q}\}$  and  $Q_i$  are given. The analysis of the second term on the right-hand side of equation (5) follows the classic modal method. It is sufficient to study the first term only. Two distinct cases are identified: (a)  $\omega = 0$  and (b)  $\omega \neq 0$ .

(1) When  $\omega = 0$ , the particular integral  $u_p$  of equation (3) is given by

$$EAu_p'' = -[1 - x/l, x/l]\{\mathbf{q}\},$$

$$EAu_p = -\left[\frac{x^2}{2} - \frac{x^3}{6l}, \frac{x^3}{6l}\right]\{\mathbf{q}\}$$

with the complementary function,

$$EAu = \left[ 1 \quad \frac{x}{l} \right] \{\mathbf{c}\} - \left[ \frac{x^2}{2} - \frac{x^3}{6l} \quad \frac{x^3}{6l} \right] \{\mathbf{q}\}, \tag{6}$$

where  $\{\mathbf{c}\}$  is a 2-vector to be determined from the boundary conditions of equations (3). Therefore,

$$\{\mathbf{c}\} = \begin{bmatrix} 0 & 0 \\ l^2 & l^2 \\ 3 & 6 \end{bmatrix} \{\mathbf{q}\}.$$

After putting back into equation (6), the deflection shape due to the distributed load is given as

$$EAu = \left[ \frac{xl}{3} - \frac{x^2}{2} + \frac{x^3}{6l}, \quad \frac{xl}{6} - \frac{x^3}{6l} \right] \{\mathbf{q}\}. \tag{7}$$

The reaction at the ends of the beam are given by

$$\{\mathbf{R}_u\} = \begin{Bmatrix} -EIu'(0) \\ EIu'(l) \end{Bmatrix} = -\frac{\ell}{6} \begin{bmatrix} 2 & 1 \\ 1 & 2 \end{bmatrix} \{\mathbf{q}\} = \frac{-1}{\rho A} [\mathbf{M}] \{\mathbf{q}\}. \tag{8}$$

Therefore, the end reactions due to the finite element type loading are proportional to the mass matrix.

(2) When  $\omega \neq 0$ , the complete solution of equation (3) is given by

$$\psi^2 EAu/l^2 = [\cos(\psi\xi), \sin(\psi\xi)] \{\mathbf{c}\} - [\mathbf{n}(0, x)] \{\mathbf{q}\}, \tag{9}$$

which consists of the complementary functions and particular integral and  $\{\mathbf{c}\}$  is to be determined by the boundary conditions, where  $\psi^2 = \omega^2 \rho A l^2 / EA$  and  $\xi = x/l$ . From the boundary conditions,

$$\{\mathbf{c}\} = \begin{bmatrix} 1 & 0 \\ -\cot\psi & \operatorname{cosec}\psi \end{bmatrix} \{\mathbf{q}\}.$$

From equation (9), the deflection shape is given by

$$\begin{aligned} \psi^2 EAu/l^2 &= [\cos(\psi x/l), \sin(\psi x/l)] \begin{bmatrix} 1 & 0 \\ -\cot\psi & \operatorname{cosec}\psi \end{bmatrix} \{\mathbf{q}\} - [\mathbf{n}(0, x)] \{\mathbf{q}\} \\ &= [\mathbf{n}(\omega, x) - \mathbf{n}(0, x)] \{\mathbf{q}\}, \end{aligned} \tag{10}$$

where  $[\mathbf{n}(\omega, x)] = [\cos\psi\xi - \cot\psi \sin\psi\xi, \operatorname{cosec}\psi \sin\psi\xi]$  is the shape function at frequency  $\omega$ . The reactions at the ends are given by

$$\begin{aligned} [\mathbf{R}_u] &= \begin{Bmatrix} -EIu'(0) \\ EIu'(l) \end{Bmatrix} = \frac{l^2}{EA\psi^2} [\mathbf{D}(\omega) - \mathbf{D}(0)] \{\mathbf{q}\} \\ &= \frac{1}{\rho A \omega^2} [\mathbf{D}(\omega) - \mathbf{D}(0)] \{\mathbf{q}\} = -\frac{[\mathbf{M}(\omega, 0)] \{\mathbf{q}\}}{\rho A}, \end{aligned} \tag{11}$$

where

$$[\mathbf{D}(\omega)] = \frac{EA\psi}{l} \begin{bmatrix} \cos \psi & -\operatorname{cosec} \psi \\ -\operatorname{cosec} \psi & \cot \psi \end{bmatrix} \tag{12}$$

is the dynamic stiffness matrix and

$$[\mathbf{M}(\omega_1, \omega_2)] = \frac{[\mathbf{D}(\omega_1) - \mathbf{D}(\omega_2)]}{\omega_2^2 - \omega_1^2} \tag{13}$$

is the mixed mass matrix [1], when  $\lim \omega \rightarrow 0$ ,

$$\lim_{\omega \rightarrow 0} \frac{1}{\rho A \omega^2} [\mathbf{D}(\omega) - \mathbf{D}(0)] = \frac{1}{\rho A} \frac{\partial}{\partial \omega^2} [\mathbf{D}(0)] = -\frac{[\mathbf{M}(0)]}{\rho A},$$

according to the Leung theorem [1]. Therefore, equation (11) degenerates to equation (8) when  $\lim \omega \rightarrow 0$ .

Finally, consider the Fourier terms of equation (5). The particular solution of

$$EIu'' + \omega^2 \rho Au = -Q_i \sin(i\pi x/l) \tag{14}$$

is given by

$$u = \frac{Q_i \sin(i\pi x/l)}{EA(i\pi^*l)^2 - \rho A \omega^2}. \tag{15}$$

Therefore, the contribution of the Fourier terms to the reaction forces is

$$\{\mathbf{R}_u\} = \begin{Bmatrix} -EAu'(0) \\ EAu'(l) \end{Bmatrix} = \frac{i\pi l Q_i}{(i^2\pi^2 - \psi^2)} \begin{Bmatrix} -1 \\ (-1)^i \end{Bmatrix}. \tag{16}$$

Finally, the total reaction is

$$\{\mathbf{R}_u\} = \begin{Bmatrix} -EAu'(0) \\ EAu'(l) \end{Bmatrix} = -\frac{[\mathbf{M}(\omega, 0)]}{\rho A} \{\mathbf{q}\} + \sum_{i=1}^n \frac{i\pi l Q_i}{(i^2\pi^2 - \psi^2)} \begin{Bmatrix} -1 \\ (-1)^i \end{Bmatrix} \tag{17}$$

for  $n$  residual modal forces.

If the load is distributed linearly, the modal decomposition is completely avoided and exact results are obtained. Classically, without using the available finite element interpolation, a uniformly distributed load is expanded by the Fourier series (1), i.e.,

TABLE 1  
Convergence of  $\sum_{i=odd} 1/i^2$  to  $\pi^2/8$

| Terms     | Value  |
|-----------|--------|
| 10        | 1.2087 |
| 100       | 1.2312 |
| 1000      | 1.2355 |
| $\pi^2/8$ | 1.2337 |

$Q_i = 4h/\pi i$ ,  $i = \text{odd}$ . The static end reactions are proportional to  $\sum 1/i^2$  and  $\sum (-1)^2/i^2$  respectively. The present method gives the analytical result  $\sum_{i=\text{odd}} 1/i^2 = \pi^2/8$  immediately. Table 1 shows that the convergence of the modal method is extremely slow.

The classical modal method requires more than 1000 terms to converge to the static solutions up to four significant figures. In the dynamic case, it converges even more slowly because of the reduced denominator. With equations (11) and (17), the following closed-form summation formula can be proved

$$\sum_{i=1,3,\dots}^{\infty} \frac{1}{i^2 - \omega^2} = \frac{\pi(\cos \omega\pi - 1)}{4\omega \sin \omega\pi}.$$

### 5. BENDING VIBRATION OF AN EULER-BERNOULLI BEAM

The governing equation of the bending harmonic vibration of an Euler-Bernoulli beam is given by

$$EIv'''' - \rho A\omega^2 v = q_v(x) \tag{18}$$

with the clamped-clamped boundary conditions

$$v(0) = v'(0) = v(l) = v'(l) = 0. \tag{19}$$

The convergence of the classical modal analysis in terms of the clamped-clamped beam eigenfunctions  $\phi_i(x)$  will be very slow if  $q(0)$ ,  $q'_v(0)$ ,  $q_v(l)$ ,  $q'_v(l) \neq 0$  due to the incompatible end conditions. The convergence to the end reactions is even slower due to the necessary repeated differentiations of the displacement to determine the forces and moments. An alternative way is to express the distributed load to

$$q_v(x) = [\mathbf{n}(0, x)]\{\mathbf{q}\} + \sum Q_i \phi_i(x). \tag{20}$$

The high convergent rate is due to the fact that the end loads have been taken care of by the finite element shape function  $[\mathbf{n}(0, x)]$  and the residual of the distributed load is accounted for in the eigenmodes. To get the reactions, two distinct cases are identified: (1)  $\omega = 0$  and (2)  $\omega \neq 0$ . The first term of equation (20) corresponding to the finite element distributed load is studied first by the dynamic stiffness method and the remaining modal forces are considered later by the classical modal analysis.

When  $\omega = 0$ , the governing equation is

$$EID^4 v = [\mathbf{n}(0, x)]\{\mathbf{q}\}, \tag{21}$$

where  $D$  is a differential operator with respect to  $x$ . The distributed load is interpolated according to the finite element interpolation as shown in Figure 1(d). The solution  $v(x)$  of equation (21) with boundary conditions (19) consists of the complementary functions and the particular integral,

$$EIv = [1 \quad x \quad x^2 \quad x^3]\{\mathbf{c}\} + D^{-4}[\mathbf{n}(0, x)]\{\mathbf{q}\}. \tag{22}$$

The constant  $\{\mathbf{c}\}$  is determined by the boundary conditions (19),

$$\{\mathbf{0}\} = EI \begin{Bmatrix} v(0) \\ v'(0) \\ v(l) \\ v'(l) \end{Bmatrix} = \begin{bmatrix} 1 & 0 & 0 & 0 \\ 0 & 1 & 0 & 0 \\ 1 & l & l^2 & l^3 \\ 0 & 1 & 2l & 3l^2 \end{bmatrix} \{\mathbf{c}\} + \begin{bmatrix} 0 & 0 & 0 & 0 \\ 0 & 0 & 0 & 0 \\ l^4/28 & l^5/252 & l^4/168 & -l^5/630 \\ 2l^3/15 & l^4/60 & l^3/30 & -l^4/120 \end{bmatrix} \{\mathbf{q}\} \quad (23)$$

from which  $\{\mathbf{c}\}$  can be determined. Substituting into equation (21) gives

$$EIv = \frac{l^4}{2520} \begin{bmatrix} 66\xi^2 - 156\xi^3 + 105\xi^4 - 21\xi^6 + 6\xi^7 \\ l(21\xi^2 - 22\xi^3 + 21\xi^4 - 14\xi^6 + 3\xi^7) \\ 39\xi^2 - 54\xi^3 + 21\xi^6 - 6\xi^7 \\ -l(9\xi^2 - 131\xi^3 + 7\xi^6 - 3\xi^7) \end{bmatrix} \{\mathbf{q}\}. \quad (24)$$

The reactions at the supports are

$$\{\mathbf{R}_v\} = EI \begin{Bmatrix} v'''(0) \\ -v'(0) \\ -v'''(l) \\ v''(l) \end{Bmatrix} = -\frac{l}{420} \begin{bmatrix} 156 & 22l & 54 & -13l \\ 22l & 4l^2 & 13l & -3l^2 \\ 54 & 13l & 156 & -22l \\ -13l & -3l^2 & -22l & 4l^2 \end{bmatrix} \{\mathbf{q}\} = \frac{-[\mathbf{M}]\{\mathbf{q}\}}{\rho A}. \quad (25)$$

Therefore, the reactions are again proportional to the mass matrix.

(b) Consider the case when  $\omega \neq 0$ . The governing equation is

$$EIv'''' - \rho A\omega^2 v = q_v(x) = [\mathbf{n}(0, x)]\{\mathbf{q}\}. \quad (26)$$

whose solution is

$$\frac{\lambda^4}{l^4} EIv = [\cos \lambda \xi \quad \sin \lambda \xi \quad \cosh \lambda \xi \quad \sinh \lambda \xi] \{\mathbf{c}\} - [\mathbf{n}(0, x)]\{\mathbf{q}\}, \quad (27)$$

where the constant  $\{\mathbf{c}\}$  is determined by the boundary conditions (19) to give the complete solution

$$\frac{\lambda^4}{l^4} EIv = [\mathbf{n}(\omega, x) - \mathbf{n}(0, x)]\{\mathbf{q}\} = \rho A\omega^2 v \quad (28)$$

or

$$v = \frac{1}{\rho A\omega^2} [\mathbf{n}(\omega, x) - \mathbf{n}(0, x)]\{\mathbf{q}\}, \quad (29)$$

in which  $\lambda^4 = \omega^2 \rho A l^4 / EI$ , and  $[\mathbf{n}(\omega, x)]$  is the dynamic shape function given by

$$[\mathbf{n}(\omega, 0)] = \begin{Bmatrix} \cos \lambda \xi \\ \sin \lambda \xi \\ \cosh \lambda \xi \\ \sinh \lambda \xi \end{Bmatrix}^T \frac{1}{2\lambda^3} \begin{bmatrix} \lambda^3 - F_4\lambda & F_2l\lambda & -F_3\lambda & F_1l\lambda \\ -F_6 & l\lambda^2 + F_4l & -F_5 & -F_3l \\ \lambda^3 + F_4\lambda & -F_2l\lambda & F_3\lambda & -F_1l\lambda \\ F_6 & l\lambda^2 - F_4l & F_5 & F_3l \end{bmatrix}, \quad (30)$$



which will degenerate to the finite element shape function when  $\omega = 0$ . The frequency functions are given in Appendix A.

The support reactions are

$$\{\mathbf{R}_v\} = EI \begin{Bmatrix} v''''(0) \\ -v'(0) \\ -v'''(l) \\ v''(l) \end{Bmatrix} = \frac{1}{\rho A \omega^2} [\mathbf{D}(\omega) - \mathbf{D}(0)] \{\mathbf{q}\} = \frac{-[\mathbf{M}(\omega, 0)] \{\mathbf{q}\}}{\rho A}, \tag{31}$$

where the dynamic stiffness matrix is

$$[\mathbf{D}(\omega)] = \frac{EI}{l} \begin{bmatrix} F_6 & & & \text{sym.} \\ -F_4 l & F_2 l^2 & & \\ F_5 & -F_3 l & F_6 & \\ F_3 l & F_1 l^2 & F_4 l & F_2 l^2 \end{bmatrix}. \tag{32}$$

Finally, the modal force part of equation (20) can be treated classically.

$$EI v_i'''' - \rho A \omega^2 v = Q_i \phi_i(x), \tag{33}$$

which gives

$$v_i(x) = Q_i \phi_i(x) / \rho A (\omega_i^2 - \omega^2), \tag{34}$$

where  $\omega_i$  and  $\phi_i(x)$  are the natural frequency and modal shape respectively.

The reaction is

$$\{\mathbf{R}_v\} = EI \begin{Bmatrix} v_i''''(0) \\ -v_i''(0) \\ -v_i''''(l) \\ v_i''(l) \end{Bmatrix} = \frac{EI Q_i}{\rho A (\omega_i^2 - \omega^2)} \begin{Bmatrix} \phi_i''(0) \\ -\phi_i''(0) \\ -\phi_i''(l) \\ \phi_i''(l) \end{Bmatrix} = \frac{\ell^4 Q_i}{\lambda_i^4 - \lambda^4} \begin{Bmatrix} \phi_i''(0) \\ -\phi_i''(0) \\ -\phi_i''(l) \\ \phi_i''(l) \end{Bmatrix}, \tag{35}$$

where  $\lambda_i^4 = \rho A \ell^4 / EI$ . Finally, the total reaction is

$$\{\mathbf{R}_v\} = \frac{-[\mathbf{M}(\omega, 0)] \{\mathbf{q}\}}{\rho A} + \sum_{i=1}^n \frac{\ell^4 Q_i}{(\lambda_i^4 - \lambda^4)} \begin{Bmatrix} \phi_i''(0) \\ -\phi_i''(0) \\ -\phi_i''(l) \\ \phi_i''(l) \end{Bmatrix} \tag{36}$$

for  $n$  residual modal forces.

Alternatively, without using the available finite element interpolation, a uniformly distributed load is expanded on to the modal space,  $Q_i = 2\lambda_i \ell (1 - (-1)^i)$  approximately for  $i > 4$ . The nodal series does not converge to the end reactions at all. For example, the shear reaction force at end 1 will be proportional to  $\sum_{i=1}^{\infty} \lambda_i^4 / (\lambda_i^4 - \lambda^4)$ , which is obviously not convergent. The exact solutions by using the finite element interpolation method can be obtained immediately.

## 6. OTHER BOUNDARY CONDITIONS

For axial vibration, the dynamic stiffness for a fixed-free bar is

$$D = -\tan \psi. \quad (37)$$

For bending vibration, there are four realistic special cases which require consideration: clamped-pinned, clamped-sliding, clamped-free and pinned-pinned.

(1) *Clamped-pinned beam*: In this case,  $v(l) = 0$ , and the dynamic stiffness matrix is

$$[\mathbf{D}(\omega)] = \frac{EI}{l^3} \begin{bmatrix} F_{11} & -F_9l & F_{10} \\ -F_9l & F_7l^2 & -F_8l \\ F_{10} & -F_8l & F_{12} \end{bmatrix}. \quad (38)$$

(2) *Clamped-sliding beam*: In this case,  $v'(l) = 0$ , and the dynamic stiffness matrix is

$$[\mathbf{D}(\omega)] = \frac{EI}{l^3} \begin{bmatrix} F_{18} & F_{19}l & F_{20}l \\ F_{19}l & F_{21}l^2 & F_{22}l^2 \\ F_{20}l & F_{22}l^2 & F_{23}l^2 \end{bmatrix}. \quad (39)$$

(3) *Clamped-free beam*: In this case,  $v(l) = v'(l) = 0$  and the dynamic stiffness matrix is

$$[\mathbf{D}(\omega)] = \frac{EI}{l^3} \begin{bmatrix} F_{17} & -F_{16}l \\ -F_{16}l & F_{15}l^2 \end{bmatrix}. \quad (40)$$

(4) *Pinned-pinned beam*: In this case,  $v(0) = v(l) = 0$ , and the dynamic stiffness matrix is

$$[\mathbf{D}(\omega)] = \frac{EI}{l^3} \begin{bmatrix} F_{14} & F_{13} \\ F_{13} & F_{14} \end{bmatrix}. \quad (41)$$

Cases (1), (3) and (4) can be constructed from Kolousek's book [6]. Case (2) is new. The frequency functions are listed in Appendix A.

## 7. GENERAL FORMULATION

The results presented in the previous sections are also valid for other structural element. A proof is given here. In order to solve the following system (a), the solutions to three more systems (b)–(d) are required.

*System (a)* is the system to be solved for the boundary reaction.

*Governing equation*

$$\mathbf{L}\mathbf{u} - \omega^2 \boldsymbol{\rho}\mathbf{u} = \mathbf{v}\mathbf{q}, \quad (42)$$

where  $\mathbf{L}$  is a linear differential operation of stiffness,  $\boldsymbol{\rho}$  is the inertia matrix,  $\mathbf{u}(x, y, z)$  is a vector function to be determined, the order of  $\mathbf{u}$  is six for a helical beam: three displacements plus three rotations;  $\mathbf{v}$  is the static shape function which is a given solution of system (b) below;  $\mathbf{q}$  is the vector value of the distributed load at the ends, i.e., the given distributed load  $\mathbf{r}(x, y, z)$  is interpolated according to  $\mathbf{r}(x, y, z) = \mathbf{v}(x, y, z)\mathbf{q}$ ;  $\mathbf{B}$  is a boundary differential operator; and  $\mathfrak{R}$  is a boundary force operator.

*Boundary conditions*

$$\mathbf{B}\mathbf{u} = \mathbf{0}. \quad (43)$$

*Reaction force*

$$\mathbf{R} = \mathfrak{R}\mathbf{u}, \quad (44)$$

which is the ultimate vector to be determined.

System (b) is a given static system with unit boundary conditions.

*Governing equation*

$$\mathbf{L}\mathbf{v} = \mathbf{0}. \quad (45)$$

*Boundary conditions*

$$\mathbf{B}\mathbf{v} = \mathbf{I}. \quad (46)$$

*Reaction force*

$$\mathbf{R}_0 = \mathfrak{R}\mathbf{v} = \mathbf{D}(0). \quad (47)$$

The last relation is derived from the fact that the boundary force is related to the boundary displacement by means of the stiffness matrix, i.e.,

$$\mathbf{R}_0 = \mathfrak{R}\mathbf{v} = \mathbf{D}(0)\mathbf{B}\mathbf{v} = \mathbf{D}(0)\mathbf{I} = \mathbf{D}(0).$$

System (c) is a given dynamic system with unit boundary conditions.

*Governing equation*

$$\mathbf{L}\Phi - \omega^2\rho\Phi = \mathbf{0}. \quad (48)$$

*Boundary conditions*

$$\mathbf{B}\Phi = \mathbf{I}. \quad (49)$$

*Reaction force*

$$\mathbf{R}_\omega = \mathfrak{R}\Phi = \mathbf{D}(\omega). \quad (50)$$

The last relation is derived from the fact that the boundary force is related to the boundary displacement by means of the stiffness matrix, i.e.,

$$\mathbf{R}_\omega = \mathfrak{R}\Phi = \mathbf{D}(\omega)\mathbf{B}\Phi = \mathbf{D}(\omega)\mathbf{I} = \mathbf{D}(\omega).$$

System (d) is a given natural mode system with clamped boundary conditions. This system is required only when the finite element interpolation is not adequate for the distributed load, i.e., when the modal analysis is needed to study the residual load after the finite element interpolation.

*Governing equation*

$$\mathbf{L}\varphi_i - \omega^2\rho\varphi_i = \mathbf{0}. \quad (51)$$

*Boundary equation*

$$\mathbf{B}\varphi_i = \mathbf{0}. \quad (52)$$

*Reaction force*

$$\mathbf{R}_i = \Re \boldsymbol{\varphi}_i. \quad (53)$$

It is to be proved that

$$\mathbf{R} = -\boldsymbol{\rho}^{-1} \mathbf{M}(\omega, 0) \mathbf{q} + \sum_{i=1}^n \frac{Q_i}{(\omega_i^2 - \omega^2)} \boldsymbol{\rho}^{-1} \Re \boldsymbol{\varphi}_i \quad (54)$$

if the distributed load is expanded according to a finite element part and a modal part

$$\mathbf{q}(x, y, z) = \mathbf{v}(x, y, z) \mathbf{q} + \sum Q_i \boldsymbol{\varphi}_i(x, y, z). \quad (55)$$

The modal part will be discussed later. Assuming that there is no residual modal component, system (a) is solved in the following manner.

Let the complementary solution be  $\boldsymbol{\Phi} \mathbf{c}$  and the particular integral integral be  $\mathbf{v} \mathbf{q}$ , where  $\mathbf{c}$  is a vector of integration constants to be determined. Substituting

$$\omega^2 \boldsymbol{\rho} \mathbf{u} = \boldsymbol{\Phi} \mathbf{c} - \mathbf{v} \mathbf{q} \quad (56)$$

into equation (42), with the help of equation (48), it can be verified that equation (56) indeed satisfies equation (42). The boundary operator can be applied to equation (56),

$$\omega^2 \boldsymbol{\rho} \mathbf{B} \mathbf{u} = \mathbf{B} \boldsymbol{\Phi} \mathbf{c} - \mathbf{B} \mathbf{v} \mathbf{q} = \mathbf{c} - \mathbf{q} = \mathbf{0} \quad (57)$$

because of equations (43), (46) and (49). That is,  $\mathbf{c} = \mathbf{q}$ . Substituting into equation (56), gives

$$\omega^2 \boldsymbol{\rho} \mathbf{u} = [\boldsymbol{\Phi} - \mathbf{v}] \mathbf{q}. \quad (58)$$

Applying the boundary force operator to equation (58) gives

$$\omega^2 \boldsymbol{\rho} \mathbf{R} = \omega^2 \boldsymbol{\rho} \Re \mathbf{u} = [\Re \boldsymbol{\Phi} - \Re \mathbf{v}] \mathbf{q} = [\mathbf{D}(\omega) - \mathbf{D}(0)] \mathbf{q}. \quad (59)$$

Therefore,

$$\mathbf{R} = \omega^{-2} \boldsymbol{\rho}^{-1} [\mathbf{D}(\omega) - \mathbf{D}(0)] \mathbf{q} = -\boldsymbol{\rho}^{-1} [\mathbf{M}(\omega, 0)] \mathbf{q}. \quad (60)$$

It only remains to solve the reactions resulting from the residual modal forces, i.e., to solve

$$\mathbf{L} \mathbf{u}_i - \omega^2 \boldsymbol{\rho} \mathbf{u}_i = Q_i \boldsymbol{\varphi}_i, \quad (61)$$

which gives

$$\mathbf{u}_i = Q_i \boldsymbol{\rho}^{-1} \boldsymbol{\varphi}_i / (\omega_i^2 - \omega^2). \quad (62)$$

Therefore, the total reaction is given by

$$\mathbf{R} = -\boldsymbol{\rho}^{-1} [\mathbf{M}(\omega, 0)] \mathbf{q} + \sum_{i=1}^n Q_i \boldsymbol{\rho}^{-1} \boldsymbol{\varphi}_i / (\omega_i^2 - \omega^2) \quad (63)$$

for  $n$  residual modal forces.

## 8. RANDOM RESPONSE

Only the finite element interpolated load for analytical solutions are now considered. The analysis of the residual modal forces can be found in textbooks [58] and will not be

discussed further. The present contribution is important as the classical modal analysis does not always converge to any solution for the support reactions which are necessary for the application of the principle of superposition in order to analyze a structure with members having distributed loads.

Let the associated deterministic load  $\mathbf{r} = \mathbf{r}(\omega, \mathbf{x}) = \mathbf{r}(\omega, x, y, z)$  be interpolated by

$$\mathbf{r} = \mathbf{r}(\omega, \mathbf{x}) = \mathbf{v}(\mathbf{x})\mathbf{q}(\omega), \quad (64)$$

where  $\mathbf{v}$  is the static finite element shape functions satisfying system (b), i.e., the static equation with unit boundary conditions and  $\mathbf{q}$  is the vector of nodal values of the distributed load  $\mathbf{r}$ . The corresponding interpolated power spectral density matrix is given by

$$\mathbf{S}_{rr}(\omega, \mathbf{x}, \mathbf{y}) = \mathbf{v}(\mathbf{x})\mathbf{S}_{qq}(\omega)\mathbf{v}^T(\mathbf{y}), \quad (65)$$

where  $\mathbf{S}_{rr}(\omega, \mathbf{x}, \mathbf{y})$  is the given fully correlated power spectral density matrix of the distributed excitation, and  $\mathbf{S}_{qq}(\omega)$  is the interpolated power spectral density matrix at the nodes obtained by curve fits. Equation (65) is obtained by taking the ensemble average of  $\mathbf{r}(\omega, \mathbf{x})\mathbf{r}^T(\omega, \mathbf{y})$ .

Specifically, for curve-fit purposes,  $\mathbf{S}_{qq}(\omega)$  may take the following form:

$$\mathbf{S}_{qq}(\omega) = \sum f_i(\omega)\mathbf{S}_{qq}^i \quad (66)$$

Equation (65) is used for the subsequent analysis. The governing equation of the response power spectral density matrix  $\mathbf{S}_{uu}(\omega, \mathbf{x}, \mathbf{y})$  corresponding to system (a) is

$$(\mathbf{L}_x - \omega^2\boldsymbol{\rho})(\bar{\mathbf{L}}_y - \omega^2\boldsymbol{\rho})\mathbf{S}_{uu} = \mathbf{S}_{rr} = \mathbf{v}(\mathbf{x})\mathbf{S}_{qq}(\omega)\mathbf{v}^T(\mathbf{y}), \quad (67)$$

where  $\mathbf{L}_x$  operates on functions of  $\mathbf{x}$  and  $\mathbf{L}_y$  operates on functions of  $\mathbf{y}$ , damping is accounted for by using complex elastic modulus and an overbar denotes complex conjugate. Corresponding to solution (58), the response power spectral density matrix is

$$\mathbf{S}_{uu}(\omega, \mathbf{x}, \mathbf{y}) = \omega^{-4}\boldsymbol{\rho}^{-1}[\boldsymbol{\Phi}(\omega, \mathbf{x}) - \mathbf{v}(\mathbf{x})]\mathbf{S}_{qq}(\omega)[\bar{\boldsymbol{\Phi}}(\omega, \mathbf{y}) - \mathbf{v}(\mathbf{y})]^T\boldsymbol{\rho}^{-1}. \quad (68)$$

Corresponding to solution (58), the reaction power spectral density matrix at the support is

$$\mathbf{S}_{RR}(\omega) = \boldsymbol{\rho}^{-1}\mathbf{M}(\omega, 0)\mathbf{S}_{qq}(\omega)\bar{\mathbf{M}}^T(\omega, 0)\boldsymbol{\rho}^{-1}. \quad (69)$$

According to the principle of superposition depicted in Figure 1, the reaction power spectral density matrix at the supports of the structural member becomes the equivalent nodal excitation power spectral density matrix on the structure. The dynamic stiffness equation

$$\mathbf{D}(\omega)\mathbf{d} = \mathbf{R} \quad (70)$$

relates the amplitude of nodal response  $\mathbf{d}$  to the nodal excitation  $\mathbf{R}$ . The power spectral density matrix of  $\mathbf{d}$  is given by

$$\mathbf{S}_{dd}(\omega) = \mathbf{D}^{-1}(\omega)\mathbf{S}_{RR}(\omega)\bar{\mathbf{D}}^{-T}(\omega). \quad (71)$$

Finally, the response power spectral density matrix of the loaded member is given by the superposition of equations (68) and (71); that is,

$$\begin{aligned} \mathbf{S}_{uu}(\omega, \mathbf{x}, \mathbf{y}) = & \omega^{-4}\boldsymbol{\rho}^{-1}[\boldsymbol{\Phi}(\omega, \mathbf{x}) - \mathbf{v}(\mathbf{x})]\mathbf{S}_{qq}(\omega)[\bar{\boldsymbol{\Phi}}(\omega, \mathbf{y}) - \mathbf{v}(\mathbf{y})]^T\boldsymbol{\rho}^{-1} \\ & + \mathbf{D}^{-1}(\omega)\boldsymbol{\rho}^{-1}\mathbf{M}(\omega, 0)\mathbf{S}_{qq}(\omega)\bar{\mathbf{M}}^T(\omega, 0)\boldsymbol{\rho}^{-1}\bar{\mathbf{D}}^{-T}(\omega), \end{aligned} \quad (72)$$

where  $\mathbf{S}_{qq}(\omega)$  is the given power spectral density matrix of the nodal values of the correlated distributed force.

If the power spectral density matrix of the distributed load is adequately represented by equation (66), the dynamic shape functions  $\Phi(\omega, \mathbf{x})$  and the dynamic stiffness matrix  $\mathbf{D}(\omega)$  are available, and the response power spectral density matrix of a continuously loaded member is given analytically in equation (72).

## 9. NUMERICAL EXAMPLES

For axial and torsional vibration of an Euler–Bernoulli beam the governing differential equations are expressed as equations (3) and (4) respectively. Some numerical examples of the procedure of solution, as outlined in sections 7 and 8 above, are presented for harmonic excitations and random loading respectively.

### 9.1. HARMONIC LOADING

For the axial vibration of an Euler–Bernoulli beam with one-dimensional harmonic finite element interpolated loading, the four steps presented in section 7 are followed to obtain a solution for the displacement and boundary reactions of the system. Solution for the residual modal forces is not considered in this section as it can be found in many textbooks [58] and can be added to the solutions in this section by means of superposition.

*Step 1.* The governing equation is

$$EIu'' + \omega^2 \rho Au = -q_u \quad \text{with } u(0) = u(l) = 0, \quad (73)$$

where the linear differential operator is  $\mathbf{L} = EI\partial/\partial x^2$ .

*Step 2.* Define a static system with governing equation

$$EIv'' = \mathbf{0} \quad (74)$$

and unit finite element boundary conditions

$$\mathbf{B}v = \mathbf{I}, \quad (75)$$

where  $\mathbf{B}$  is a boundary differential operator. Solving equation (74) and imposing unit finite element boundary conditions (75) gives

$$v = [1 - x/l, x/l] = [1 - \xi, \xi], \quad (76)$$

where  $\xi$  is a dimensionless co-ordinate.

*Step 3.* Define a dynamic system with governing equation

$$EI\Phi'' + \omega^2 A\Phi = \mathbf{0} \quad (77)$$

and unit finite element boundary conditions

$$\mathbf{B}\Phi = \mathbf{I}. \quad (78)$$

Solving equation (77) and imposing unit finite element boundary conditions (78), gives

$$\Phi = [\cos \psi \xi - \cot \psi \sin \psi \xi, \quad \operatorname{cosec} \psi \sin \psi \xi]. \quad (79)$$

Step 4. A solution for the complete system in Step 1 above could be obtained from component solutions in Steps 2 and 3. Equation (58) gives

$$\begin{aligned}
 -\omega^2 \rho A \mathbf{u} &= [\Phi - \mathbf{v}] \mathbf{q} \\
 &= [\cos \psi \xi - \cot \psi \sin \psi \xi - (1 - \xi), \quad \operatorname{cosec} \psi \sin \psi \xi - \xi] \mathbf{q}.
 \end{aligned}
 \tag{80}$$

which is the displacement solution for the axial vibration of an Euler-Bernoulli beam.

9.2. RANDOM LOADING

For an axially vibrating beam with one-dimensional random finite element interpolated loading, the deterministic load can be expressed as

$$\mathbf{r} = \mathbf{r}(\omega, \mathbf{x}) = \mathbf{r}(\omega, \mathbf{y}) = \mathbf{r}(\omega, x)
 \tag{81}$$

and it can be interpolated by

$$\mathbf{r} = \mathbf{r}(\omega, x) = \mathbf{v}(x) \mathbf{q}(\omega) = \mathbf{n}(0, x) \mathbf{q}(\omega),
 \tag{82}$$

where  $\mathbf{N}(0, x) = [1 - x/l, x/l]$  is the finite element shape function matrix. Also

$$\Phi(\omega, \mathbf{x}) = \Phi(\omega, \mathbf{y}) = \Phi(\omega, x) = \mathbf{N}(\omega, x),
 \tag{83}$$

where  $\mathbf{n}(\omega, x) = [\cos \psi \xi - \cot \psi \sin \psi \xi, \operatorname{cosec} \psi \sin \psi \xi]$  is the shape function at frequency  $\omega$ . The interpolated power spectral density matrix given in equation (65) can be reduced to

$$\mathbf{S}_{rr}(\omega, x) = \mathbf{n}(0, x) \mathbf{S}_{qq}(\omega) \mathbf{n}^T(0, x),
 \tag{84}$$

where  $\mathbf{S}_{qq}(\omega)$  is the given power spectral density matrix of the nodal correlated distributed force defined in equation (66). If damping is neglected in the system, the response power spectral density matrix is, from equation (68),

$$\mathbf{S}_{uu}(\omega, x) = \omega^{-4} \boldsymbol{\rho}^{-1} [\mathbf{n}(\omega, x) - \mathbf{n}(0, x)] \mathbf{S}_{qq}(\omega) [\mathbf{n}(\omega, x) - \mathbf{n}(0, x)]^T \boldsymbol{\rho}^{-1},
 \tag{85}$$

where  $\bar{\Phi}(\omega, \mathbf{y}) = \Phi(\omega, \mathbf{y}) = \mathbf{n}(\omega, x)$  as the complex conjugate of a real matrix equals itself. The reaction power spectral density matrix at the supports is, from equation (69),

$$\begin{aligned}
 \mathbf{S}_{RR}(\omega) &= \boldsymbol{\rho}^{-1} \mathbf{M}(\omega, 0) \mathbf{S}_{qq}(\omega) \mathbf{M}^T(\omega, 0) \boldsymbol{\rho}^{-1} \\
 &= \boldsymbol{\rho}^{-1} [\mathbf{D}(\omega) - \mathbf{D}(0)] \mathbf{S}_{qq}(\omega) [\mathbf{D}(\omega) - \mathbf{D}(0)]^T \boldsymbol{\rho}^{-1} / \omega^{-4},
 \end{aligned}
 \tag{86}$$

where  $[\mathbf{M}(\omega_1, \omega_2)] = [\mathbf{D}(\omega_1) - \mathbf{D}(\omega_2)] / (\omega_2^2 - \omega_1^2)$ , as presented in equation (13), is the mixed mass matrix and  $[\mathbf{D}(\omega)]$  is the dynamic stiffness matrix. For an Euler-Bernoulli beam,

$$[\mathbf{D}(\omega)] = \frac{EI\psi}{l} \begin{bmatrix} \cot \psi & -\operatorname{cosec} \psi \\ -\operatorname{cosec} \psi & \cot \psi \end{bmatrix}$$

is solved and presented in equation (12). Therefore, the response power spectral density matrix of a loaded Euler-Bernoulli beam can be obtained as

$$\begin{aligned}
 \mathbf{S}_{uu}(\omega, x) &= \omega^{-4} \boldsymbol{\rho}^{-1} [\mathbf{n}(\omega, x) - \mathbf{n}(0, x)] \mathbf{S}_{qq}(\omega) [\mathbf{n}(\omega, x) - \mathbf{n}(0, x)]^T \boldsymbol{\rho}^{-1} \\
 &\quad + \mathbf{D}^{-1}(\omega) \boldsymbol{\rho}^{-1} [\mathbf{D}(\omega) - \mathbf{D}(0)] \mathbf{S}_{qq}(\omega) [\mathbf{D}(\omega) - \mathbf{D}(0)]^T \boldsymbol{\rho}^{-1} \mathbf{D}^{-1}(\omega) / \omega^4.
 \end{aligned}
 \tag{87}$$

## 10. CONCLUSION

The dynamic stiffness method has been extended to distributed loads. If the distributed load can be interpolated by the finite element shape functions, exact solutions are possible. It is found that the classical modal analysis fails to obtain support reactions of an Euler–Bernoulli beam under uniformly distributed load while the present method can handle the problem easily. Both deterministic and random loads are considered. The present method analytically solves for the response power spectral density matrix for heavily damped structures through complex modulus excited by fully correlated loads.

## ACKNOWLEDGMENT

The research is supported by an U.K. EPSRC grant on the dynamic reduction methods.

## REFERENCES

1. A. Y. T. LEUNG 1993 *Dynamic Stiffness and Substructures*. London: Springer-Verlag.
2. F. W. WILLIAMS and W. H. WITTRICK 1971 *Quarterly Journal of Mechanics and Applied Mathematics* **24**, 263–284. A general algorithm for computing natural frequencies of elastic structures.
3. V. KOLOUSEK 1941 *Ingenieur Archiv* **12**, 363–370. Anwendung des Gesetzes der virtuellen verschiebungen und des reziprozitatssatzes in der stabwerksdynamik.
4. V. KOLOUSEK 1954 *Dynamics of Civil Engineering Structures* Prague (in Czech).
5. V. KOLOUSEK 1962 *Buletinul Institutului Politehnic*, DIN IASI, Serie NOUA, Tomul VIII(XII), Fasc. 3–4. Vibrations of continuous and multistorey rigid frames.
6. V. KOLOUSEK 1973 *Dynamics in Engineering Structures*. London: Butterworths.
7. B. A. AKESSON 1976 *International Journal for Numerical Methods in Engineering* **10**, 1221–1231. PFVIBAT — a computer program for plane frame vibration analysis by an exact method.
8. R. E. GASKELL 1943 *Quarterly Journal of Applied Mathematics* **1**, 237–249. On moment balancing in structural dynamics.
9. RAITHEL 1952 *Giornale del Genio Civile* **90**, 629–635. La dinamica dei sistemi solidali, Nota I: vibrazioni libere dei sistemi a nodi spostabili.
10. RAITHEL 1952 *Giornale del Genio Civile* **90**, 716–721. La dinamica dei sistemi solidali, Nota I: vibrazioni libere dei sistemi a nodi spostabili.
11. A. S. VELETSON and N. M. NEWMARK 1955 *Proceedings of the American Society of Civil Engineers* **81**, paper #735, 1–37. Natural frequencies of continuous flexural members.
12. G. L. ROGERS 1959 *Dynamics of Framed Structures*. New York: Wiley.
13. M. E. MOHSIN and E. A. SADEK 1968 *The Structural Engineering* **46**, 345–351. The distributed mass-stiffness technique for the dynamic analysis of complex frameworks.
14. I. D. ARMSTRONG 1968 *International Journal of Mechanical Sciences* **10**, 43–55. The natural frequencies of Grillages.
15. F. Y. CHENG 1970 *Journal of Structural Engineering Division American Society of Civil Engineers* **96**, 551–571. Vibrations of Timoshenko beams and frameworks.
16. P. SWANNEL 1973 *Theory and Practise in Finite Element Structural Analysis*, 289–303. Tokyo: University of Tokyo Press. Automatic computation of the natural frequencies of structural frames using an exact matrix technique.
17. D. AFOLABI 1987 *Computers and Structures* **26**, 1039–1040. Linearization of the quadratic eigenvalue problem.
18. B. A. AKESSON and H. TAGNFORS 1980 Pub. #27. *Division of Solid Mechanics, Chalmers University of Technology, Gothenburg*. SFVIBAT—a computer program for space frame vibration analysis.
19. B. A. AKESSON, H. TAGNFORS, R. LUNDEN and O. FRIBERG 1987 Pub. #29. *Division of Solid Mechanics, Chalmers University of Technology, Gothenburg*. SFVIBAT-DAMP—a computer program for damped space frame vibration analysis.



20. J. R. BANERJEE and F. W. WILLIAMS 1985 *International Journal for Numerical Methods in Engineering* **21**, 2289–2302. Exact Euler–Bernoulli dynamic stiffness matrix for a range of tapered beams.
21. M. D. CAPRON and F. W. WILLIAMS 1988 *Journal of Sound and Vibration* **124**, 453–466. Exact dynamic stiffness for an axially loaded uniform Timoshenko member embedded in an elastic medium.
22. Y. H. CHEN 1987 *Earthquake Engineering Structural Dynamics* **15**, 391–402. General dynamic stiffness matrix of a Timoshenko beam for transverse vibrations.
23. Y. H. CHEN 1988 *Journal of Ship Research* **32**, 177–185. General dynamic shape functions and stiffness matrix of Timoshenko beam and their application to structure-borne noise on ships.
24. G. CURTI, F. RAFFA and F. VATTA 1991 *STLE Tribology Translations* **34**, 81–85. The dynamic stiffness matrix method in the analysis of rotating systems.
25. M. EISENBERGER 1990 *American Institute of Aeronautics and Astronautics Journal* **28**, 1105–1109. Exact static and dynamic stiffness matrices for general variable cross section members.
26. M. EISENBERGER 1991 *Computers and Structures* **41**, 75–772. Exact solutions for general variable cross-section members.
27. P. O. FRIBERG 1983 *International Journal for Numerical Methods in Engineering* **19**, 479–493. Coupled vibrations of beams—an exact dynamic element stiffness matrix.
28. P. O. FRIBERG 1985 *International Journal for Numerical Methods in Engineering* **21**, 1205–1228. Beam element matrices derived from Vlasovs theory of open thin-walled elastic beams.
29. W. L. HALLAUER Jr, R. Y. L. LIU 1982 *Journal of Sound and Vibration* **85**, 105–113. Beam bending-torsion dynamic stiffness method for calculating of exact vibration modes.
30. H. HENCKY 1947 *Ing.-Arch.* **16**. Uber die berucksichtigung der schubverzerrungein in ebenen platten.
31. A. Y. T. LEUNG 1976 *Ph.D. Thesis, University of Aston, Birmingham, U.K.* Dynamics of structural vibrations by frequency-dependent matrices and modal analysis.
32. A. Y. T. LEUNG 1978 *International Journal for Numerical Methods in Engineering* **12**, 1705–1715. An accurate method of dynamic condensation in structural analysis.
33. A. Y. T. LEUNG 1979 *International Journal for Numerical Methods in Engineering* **14**, 1241–1256. An accurate method of dynamic substructuring with simplified computation.
34. A. Y. T. LEUNG 1980 *Proceedings of Conference on Advances in Structural Dynamics, University of Southampton*, 101–108. Accelerated converging methods in structural response analysis.
35. A. Y. T. LEUNG 1985 *Journal of Sound and Vibration* **98**, 337–347. Dynamic stiffness method for exponentially varying harmonic excitation of continuous systems.
36. A. Y. T. LEUNG 1987 *Dynamics and Stability of Systems* **2**, 125–137. Dynamic stiffness and response analysis.
37. A. Y. T. LEUNG 1988 *Journal of Sound and Vibration* **124**, 249–267. Dynamic stiffness analysis of follower force.
38. A. Y. T. LEUNG 1989 *International Journal of Analytical and Experimental Modal Analysis* **43**, 77–82. Dynamic stiffness and nonconservative modal analysis.
39. A. Y. T. LEUNG 1990 *Communications in Applied Mathematics* **6**, 401–409. Perturbed general eigensolutions.
40. A. Y. T. LEUNG 1991 *Finite Elements in Analysis and Design* **9**, 23–32. Exact stiffness matrix for twisted helix beam.
41. R. LUNDE and B. AKESSON 1983 *International Journal for Numerical Methods in Engineering* **19**, 431–449. Damped 2nd order Rayleigh–Timoshenko beam vibrating in space — an exact dynamic member stiffness matrix.
42. B. A. OVUNC 1972 *Publ IABSE (Zurich)* **32**, 137–154. Dynamic analysis of frameworks by frequency dependent stiffness matrix approach.
43. B. A. OVUNC 1974 *Computers and Structures* **4**, 1061–1089. Dynamics of frameworks by continuous mass method.
44. W. D. PILKEY 1987 *Proceedings of 28th Structural Dynamics and Materials Conference*, Paper no. 87–0815, Part 2a, 296–299. A new look at frequency-dependent structural matrices to achieve accurate free dynamics analyses.
45. T. H. RICHARDS and Y. T. LEUNG 1977 *Journal of Sound and Vibration* **55**, 363–376. An accurate method in structural vibration analysis.
46. F. W. WILLIAMS and K. KENNEDY 1987 *Earthquake Engineering and Structural Dynamics* **15**, 133–136. Exact dynamic member stiffnesses for a beam on an elastic foundation.
47. F. W. WILLIAMS and W. H. WITTRICK 1983 *Journal of Structural Engineering* **109**, 169–187. Exact buckling and frequency calculations survEYED.

48. Y. S. ZHANG, D. P. GAO and X. P. WU 1989 *Applied Mathematical Methods* **10**, 1151–1162. Dynamic stiffness matrix for the finite annular plate element.
49. N. J. FERGUSSON 1991 *Ph.D. Thesis, University of Virginia, Virginia, U.S.A.* The free and forced vibrations of structures using the finite dynamic element method.
50. A. Y. T. LEUNG and W. E. ZHOU 1993 *Shocks and Vibration* **1**, 77–88. Dynamic stiffness analysis of curved thin-walled beams.
51. A. Y. T. LEUNG and W. E. ZHOU 1993 *Proceedings of the 3rd International Offshore and Polar Engineering Conference*, 482–488. Dynamic Stiffness analysis of circular cylindrical shells.
52. A. Y. T. LEUNG and W. E. ZHOU 1995 *Journal of Sound and Vibration* **181**, 447–456. Dynamic stiffness analysis of non-uniform Timoshenko beams.
53. A. Y. T. LEUNG and W. E. ZHOU 1995 *Computers and Structures* **56**, 577–588. Dynamic stiffness analysis of axially loaded non-uniform Timoshenko columns.
54. A. Y. T. LEUNG and T. C. KWOK 1995 *Thin Walled Structures* **21**, 43–64. Dynamic stiffness analysis of toroidal shell.
55. A. Y. T. LEUNG and W. E. ZHOU 1996 *Thin Walled Structures* **25**, 109–134. Dynamic stiffness analysis of laminated composite plates.
56. M. EIGENBERGER 1995 *Thin-Walled Structures* **21**, 93–105. Nonuniform torsional analysis of variable and open cross-section bars.
57. M. EIGENBERGER 1997 *Thin-Walled Structures* **28**, 269–278. Torsional vibrations of open and variable cross-section bars.
58. D. E. NEWLAND 1993 *An Introduction to Random Vibrations, Spectral and Wavelet Analysis*. Essex: Longman.

#### APPENDIX A: FREQUENCY FUNCTIONS

$$F_1 = \lambda(\sinh \lambda - \sin \lambda)/(\cosh \lambda \cos \lambda - 1),$$

$$F_2 = -\lambda(\cosh \lambda \sin \lambda - \sinh \lambda \cos \lambda)/(\cosh \lambda \cos \lambda - 1),$$

$$F_3 = -\lambda^2(\cosh \lambda - \cos \lambda)/(\cosh \lambda \cos \lambda - 1),$$

$$F_4 = \lambda^2 \sinh \lambda \sin \lambda / (\cosh \lambda \cos \lambda - 1),$$

$$F_5 = \lambda^3(\sinh \lambda + \sin \lambda)/(\cosh \lambda \cos \lambda - 1),$$

$$F_6 = -\lambda^3(\cosh \lambda \sin \lambda + \sinh \lambda \cos \lambda)/(\cosh \lambda \cos \lambda - 1),$$

$$F_7 = 2\lambda \sinh \lambda \sin \lambda / (\cosh \lambda \sin \lambda - \sinh \lambda \cos \lambda),$$

$$F_8 = \lambda^2(\sinh \lambda + \sin \lambda)/(\cosh \lambda \sin \lambda - \sinh \lambda \cos \lambda),$$

$$F_9 = -\lambda^2(\cosh \lambda \sin \lambda + \sinh \lambda \cos \lambda)/(\cosh \lambda \sin \lambda - \sinh \lambda \cos \lambda),$$

$$F_{10} = -\lambda^3(\cosh \lambda + \cos \lambda)/(\cosh \lambda \sin \lambda - \sinh \lambda \cos \lambda),$$

$$F_{11} = \lambda^3(2\cosh \lambda \cos \lambda)/(\cosh \lambda \sin \lambda - \sinh \lambda \cos \lambda),$$

$$F_{12} = \lambda^3(\cosh \lambda \cos \lambda + 1)/(\cosh \lambda \sin \lambda - \sinh \lambda \cos \lambda),$$

$$F_{13} = -\lambda^3(\sinh \lambda - \sin \lambda)/(2\sinh \lambda \sin \lambda),$$

$$F_{14} = -\lambda^3(\cosh \lambda \sin \lambda - \sinh \lambda \cos \lambda)/(2\sinh \lambda \sin \lambda),$$

$$F_{15} = -\lambda(\cosh \lambda \sin \lambda - \sinh \lambda \cos \lambda)/(\cosh \lambda \cos \lambda + 1),$$

$$F_{16} = \lambda^2(\sinh \lambda \sin \lambda)/(\cosh \lambda \cos \lambda + 1),$$

$$F_{17} = -\lambda^3(\cosh \lambda \sin \lambda + \sinh \lambda \cos \lambda)/(\cosh \lambda \cos \lambda + 1),$$

$$F_{18} = -2\lambda^3 \sin \lambda \sinh \lambda/(\cosh \lambda \sin \lambda + \cos \lambda \sinh \lambda),$$

$$F_{19} = \lambda^2(\cos \lambda \sinh \lambda - \cos \lambda \sin \lambda)/(\cosh \lambda \sin \lambda + \cos \lambda \sinh \lambda),$$

$$F_{20} = \lambda^2(\sin \lambda - \sinh \lambda)/(\cosh \lambda \sin \lambda + \cos \lambda \sinh \lambda),$$

$$F_{21} = 2\lambda \cos \lambda \cosh \lambda/(\cosh \lambda \sin \lambda + \cos \lambda \sinh \lambda),$$

$$F_{22} = -\lambda(\cos \lambda + \cosh \lambda)/(\cosh \lambda \sin \lambda + \cos \lambda \sinh \lambda),$$

$$F_{23} = \lambda(1 + \cos \lambda \cosh \lambda)/(\cosh \lambda \sin \lambda + \cos \lambda \sinh \lambda).$$